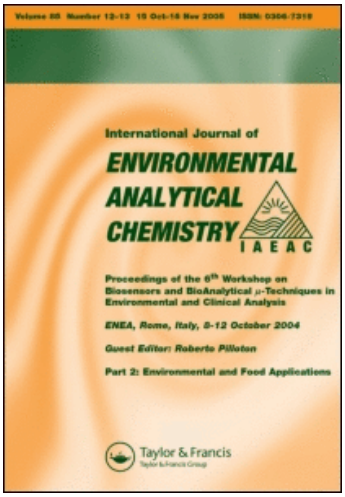

International Journal of Environmental Analytical Chemistry
Publication details, including instructions for authors and subscription information:
http://www.informaworld.com/smpp/title~content=t713640455

Use of electrochemical impedance spectroscopy to characterise the physical properties of *ex situ* reconstructed sea surface microlayer

Sanja Frka[a]; Andrew Nelson[b]; Zlatica Kozarac[a]
[a] Centre for Marine and Environment Research, Rudjer Bošković Institute, 10002 Zagreb, Croatia [b] Centre for Self Organising Molecular Systems, School of Chemistry, University of Leeds, LS2 9JT Leeds, UK

To cite this Article Frka, Sanja , Nelson, Andrew and Kozarac, Zlatica(2006) 'Use of electrochemical impedance spectroscopy to characterise the physical properties of *ex situ* reconstructed sea surface microlayer', International Journal of Environmental Analytical Chemistry, 86: 5, 325 — 335
To link to this Article: DOI: 10.1080/03067310500227852
URL: http://dx.doi.org/10.1080/03067310500227852

Intern. J. Environ. Anal. Chem.
Vol. 86, No. 5, 20 April 2006, 325–335

Taylor & Francis
Taylor & Francis Group

Use of electrochemical impedance spectroscopy to characterise the physical properties of *ex situ* reconstructed sea surface microlayer

SANJA FRKA†, ANDREW NELSON*‡ and ZLATICA KOZARAC†

†Centre for Marine and Environment Research, Rudjer Bošković Institute, 54 Bijenička, 10002 Zagreb, Croatia
‡Centre for Self Organising Molecular Systems, School of Chemistry, University of Leeds, LS2 9JT Leeds, UK

(*Received 24 January 2005; in final form 13 June 2005*)

The objective of this work was to develop electrochemical impedance spectroscopy (EIS) to characterise the physical properties of the sea surface microlayer (***ssm***). Samples from Lake Rogoznica in Croatia were extracted by *n*-hexane and dichloromethane (dcm) respectively and transferred to mercury electrodes. The EIS results were compared with those of a model phospholipid, dioleoyl phosphatidylcholine (DOPC) which forms near defect-free monolayers on a mercury surface. The ***ssm*** extracts formed inhomogeneous monolayers on the mercury surface and the dcm ***ssm*** extract monolayer showed greater surface roughness than the hexane ***ssm*** extract. The hexane ***ssm*** extract introduced defects and a greater surface roughness into mixed DOPC-***ssm*** extract monolayers than the dcm ***ssm*** extract due to the lower compatibility of the non-polar hexane extract with the DOPC than that of the polar ***ssm*** extract. In addition, the dcm ***ssm*** component in the mixed DOPC-***ssm*** monolayer showed an association with pyrene added to the solution.

Keywords: Sea surface microlayer; Electrochemical impedance spectroscopy; Monolayers

1. Introduction

The sea surface microlayer (***ssm***) represents a distinctive and complex marine environment where unique processes such as wind stress, water transpiration, solar energy flux and atmospheric inputs take place. It is derived from multiple sources and is composed of different natural and anthropogenic organic substances due to its surfactant nature, its hydrophobic properties and association with particles and its role in vertical diffusion mechanisms and bubble scavenging. In the surface microlayer in coastal environments high concentrations of toxic pollutants are also often found. In this area large vertical gradients exist and physical, chemical and biological properties are most altered relative to subsurface water at ~50 cm depth. Since the air–sea exchange

*Corresponding author. Fax: +44-113-6452. Email: andrewn@chem.leeds.ac.uk

International Journal of Environmental Analytical Chemistry
ISSN 0306-7319 print: ISSN 1029-0397 online © 2006 Taylor & Francis
DOI: 10.1080/03067310500227852

of gaseous particulate material, heat and momentum is mediated by the surface microlayer, the investigation of its physicochemical properties is of fundamental importance in marine environmental protection and global climate change [1].

The purpose of this work is to develop electrochemical impedance spectroscopy (EIS) as a technique to characterise the physical properties of ***ssm***. EIS has already been used successfully to characterise the structure and properties of phospholipid layers on mercury electrodes [2, 3]. As a result it was considered appropriate to extend these techniques to the study of samples of ***ssm*** transferred to the mercury surface. The investigations were carried out using ***ssm*** which was extracted and reconstituted with the aim of developing the techniques and the preliminary characterisation of the ***ssm***. Particular attention was paid in this study to the comparison of the properties of the ***ssm*** extracts and those of monolayers of dioleoyl phosphatidylcholine (DOPC) which form near defect-free monolayers on the mercury surface. The EIS of mixtures of DOPC and the extracts was also studied to assess the departure from defect-free monolayer behaviour of the ***ssm*** extracts. The development of EIS to assay the properties of the ***ssm*** is important since EIS combined with an appropriate electrochemical system can be used in future studies as an *in situ* technique. Before this is possible, it is necessary to relate the properties of the EIS signal to characteristics of the ***ssm***.

A preliminary series of experiments were also carried out looking at the interaction of pyrene and promethazine in solution with the ***ssm*** extracts reconstituted as mixed monolayers within the host monolayer DOPC. The interactions were carried out within a host DOPC monolayer in order to maintain a similar monolayer structure for each interaction respectively. The rationale for studying these compounds was as follows. Pyrene is a non-polar four membered polycyclic aromatic hydrocarbon and promethazine is an amphiphilic three membered surfactant. Accordingly the compounds are representative of non-polar aromatic and polar surfactant pollutant compounds respectively which can accumulate in aquatic microlayers.

2. Experimental

2.1 *Collection, pre-treatment and physical properties of the sample*

The ***ssm*** samples were collected from the small Middle Adriatic eutrophic salt-lake Lake Rogoznica during October 2003. A Garrett 16-mesh stainless steel screen, which collects the top 100–400 μm layer was used for microlayer sampling [4]. Surface microlayer samples (600 cm^3) were extracted by *n*-hexane and dichloromethane (dcm) organic solvents (p.a. grade, Kemika, Croatia). After repeated extractions, combined extracts were evaporated in a rotary evaporator. Dichloromethane extracted microlayer and hexane extracted microlayer are termed dcm ***ssm*** and hexane ***ssm*** respectively. The dried extracts were dissolved again in the corresponding organic solvent and analysed as *ex situ* reconstructed microlayers.

The content of surface active substances in the original microlayer sample was determined on the basis of the capacity current measurements using *ac* voltammetry, as described in detail in previous papers [5]. Surfactant activity is expressed in terms of the equivalent of the non-ionic surfactant tetra-octylphenolethoxylate (Triton-X-100 in mg dm^{-3}) which in the microlayer samples equals 1.30 mg dm^{-3} [5]. The surfactant activity of the sub-phase water was 0.27 mg dm^{-3}. The degree to which the microlayer

sample is enriched in chemical or biological species is usually assessed through the enrichment factor which is the ratio of microlayer and bulk concentration. The enrichment factor was 4.8, which is a larger enrichment factor than average, indicating that the sea surface microlayer sample was very rich in surface active material. The concentration of dissolved organic carbon (DOC) was also estimated and was 3.31 mg dm^{-3} for the original microlayer sample and 2.73 mg dm^{-3} for the subsurface water.

Measurements of surface pressure-area (π–A) isotherms enable the characterisation of the states and elastic properties of natural microlayers. Surface pressure-area (π–A) isotherms were measured in a Teflon trough enclosed in a tight box and thermostatted. A Wilhelmy balance was used to measure the surface pressure. The compression velocity was 60 cm^2 min^{-1} [6]. From the π–A isotherms, the thermodynamic parameter describing the viscoelastic properties of the monolayers (compressional modulus C_s^{-1}) was calculated [7]. The inverse value of the compressional modulus is the compressibility and higher values are obtained from more compressible films.

The estimation of the compressibility values of sea surface microlayers is crucial in the evaluation of the environmental consequences of a surfactant modified air–sea interface. This is because aquatic natural organic films affect air–water gas exchange through the hydrodynamic effect of a film arising from the viscoelastic properties of a surface layer. The compressibility value for the original microlayer sample was 0.058 mm N^{-1}. Compressibility values for microlayer samples from Rogoznica lake analysed in a three-year period were in the range from 0.050–0.083 mm N^{-1} [8]. which is higher than the value for pure lipid compounds, showing a complex composition of natural surface films. For comparison, it is known that the compressibilities of the monolayers of cholesterol and stearic acid are 0.0012 and 0.0019 mm N^{-1}, of some proteins between 0.015 and 0.03 mm N^{-1}, of sedimentary humic acid in different molecular weight range between 0.024 and 0.036 mm N^{-1} [9], of non-ionic surfactant polyoxyethylene(6)dodecanol, 0.056 mm N^{-1}, of chlorophyll, 0.021 mm N^{-1}, of vitamin A, 0.019 mm N^{-1} and of sodium dodecylbenzenesulphonate 0.017 mm N^{-1} [10].

2.2 *Apparatus and materials*

An Autolab system, FRA and PGSTAT 30 interface (Ecochemie, Utrecht, The Netherlands), controlled with Autolab software, was used in all the electrochemical experiments. The experiments were performed in a standard three electrode cell which was temperature controlled at 25°C. An Ag/AgCl, 3.5 mol dm^{-3} KCl reference electrode with a porous sintered glass frit separating the 3.5 mol dm^{-3} KCl solution from the electrolyte served as reference electrode and all potentials in this article are quoted relative to this. A platinum bar served as counter electrode and the reference and counter electrodes were located on either side of the working electrode. A solution resistance of around 280–300 ohms was recorded for the cell. Diagnostic plots of the impedance data showed it to be that of an *RC* series circuit as before [2, 3]. There was a distinct absence of instability at high frequencies and for this reason, the use of a fourth pseudo-reference electrode was not considered necessary at this stage. The electrochemical cell and screened cables were contained in an aluminium Faraday cage.

The electrolyte, KCl (0.1 mol dm^{-3}) was prepared from Analar KCl (Fisher Chemicals Ltd) calcined at 600°C using 18.2 MΩ MilliQ water with added 0.01 mol dm^{-3} phosphate (E. Merck, Suprapur) buffer. A blanket of argon gas was maintained above the fully

deaerated electrolyte during all experiments. Mixtures of DOPC, DOPC + hexane ***ssm***, DOPC + dcm ***ssm*** were prepared by mixing the ***ssm*** with phospholipids in specified weight fraction in a working solution. These DOPC + ***ssm*** mixtures are referred to throughout the text as DOPC-weight fraction ***ssm***. 13 μdm^3 of a 2 mg cm^{-3} solution of the ***ssm***, DOPC and DOPC-***ssm*** mixture in pentane (HPLC grade, Fisher Scientific Chemicals Ltd) was spread at the argon-electrolyte interface in the electrochemical cell as appropriate [11, 12]. The working solution of DOPC was obtained by dilution of the 50 mg cm^{-3} stock solution (Avanti Lipids). A fresh mercury drop (area, $A = 0.0088\,cm^2$) was coated with the ***ssm***, DOPC and DOPC-***ssm*** from the argon-electrolyte interface prior to each series of experiments.

To investigate the interaction of the monolayers with pyrene and promethazine in solution the pyrene (SIGMA) and promethazine (ALDRICH) were dissolved in acetone to give $\sim 13 \times 10^{-3}$ mol dm^{-3} stock solution. Aliquots were added to the electrolyte to give 4×10^{-7} mol dm^{-3} concentration of pyrene and promethazine respectively after the monolayer had been spread and electrochemically monitored. The electrolyte was then stirred for 5 min and the resultant monolayer at the gas–water interface was deposited on the mercury.

2.3 *Electrochemical impedance*

Measurements of capacity (C) *versus* potential ($-E$) for the monolayer coated electrode were carried out by measuring the imaginary impedance (Z'') at potentials between -0.2 and -1.05 V at a frequency (f) of 75 Hz with 0.005 V rms. These measurements were performed at 0.025 V intervals at potentials between -0.2 and -0.8 V and at -0.005 V intervals at potentials between -0.8 and -1.05 V. Capacitance (C_d) was calculated from the Z'' value using the equation $C_d = (1/Z''\omega)$ where ω is the angular frequency ($=2\pi f$) assuming RC series behaviour of the cell.

Measurements of the impedance (Z) *versus* frequency of the electrode systems using frequencies logarithmically distributed from 65 000 to 0.1 Hz, 0.005 V rms at potentials of -0.4 V were carried out on the coated electrode systems. The experimental conditions for the measurement of impedance are listed in the following. For one measurement, one cycle was used except when the cycle was less than one second, in which case, the measurement time was one second. In order to reach steady state, ten cycles were used except when ten cycles lasted more than three seconds, in which case, three seconds were used. Each frequency scan took 5 min with the potential continually applied commencing with the highest frequency. These time intervals are a compromise in providing sufficient time to carry out the measurement and reaching a steady state, whilst still enabling all the experiments to be done within a specified time period on one monolayer without altering the structure of the layer. No significant difference in the spectra was noted when longer equilibration periods were used before each experiment. The impedance data were transformed to the complex capacitance plane and the complex capacitance axes were expressed as $\mathrm{Re}(Y\omega^{-1})$ and $\mathrm{Im}(Y\omega^{-1})$ respectively. This was done using the EXCEL (Microsoft) spreadsheet. Curve fitting of the data was carried out using IGOR (Wavemetrics) in the same way as described previously [2, 3].

Due to the absence of any electroactive component, the simplest equivalent circuit model is the uncompensated solution resistance (R_u) of the cell and the capacitance (C) of the monolayer coated electrode in series [13]. R_u can be determined

by extrapolating the *Im Z* versus *Re Z* plot to the *Re Z* axis [14]. In the complex capacitance plane, values of $Re\,Y\omega^{-1}$ were plotted against $Im\,Y\omega^{-1}$ for all values of frequency [14–16]. For a series *RC* circuit, the $Re\,Y\omega^{-1}$ versus $Im\,Y\omega^{-1}$ plots gives a single semicircle for the *RC* element, where the capacitor has no frequency dispersion. The extrapolation of this semicircle to the $Im\,Y\omega^{-1}$ axis at low frequency gives the zero frequency capacitance (*ZFC*) [14–16] of the *RC* circuit which is therefore an empirical quantity and is the monolayer capacitance (*C*). Any additional elements to the *RC* semicircle at lower frequencies will correspond to properties of the monolayer. Further, if the semicircle representing the *RC* element is not perfect [17], the non-ideality of the capacitor is indicated. This can be due to dielectric relaxations coupled to the *RC* charging process and to additional circuit elements at the interface between the capacitor and the solution resistance [18]. Inhomogeneities in the monolayer give rise to a low frequency relaxation of the capacitor [2–3]. This is seen as an additional capacitative element which appears to the right of the *RC* semicircle in the complex capacitance plane plot [2, 3] (see figure 1a).

Some of the impedance data were fitted to equation (1) below as done previously [2, 3].

$$Y = \frac{1}{R + 1/\left((i\omega)^{\beta}\omega_o^{1-\beta}[((C_s - C_{inf})/(1 + (i\omega\tau)^{\alpha})) + C_{inf}]\right)} \tag{1}$$

In equation (1), Y is the admittance, R is equivalent to the uncompensated solution resistance (R_u), C_{inf} is equivalent to the zero frequency capacitance (*ZFC*) of the monolayer, $C_s - C_{inf}$ is the additional low frequency capacitative element with relaxation time constant, (τ), α is the coefficient which represents the distribution of time constants around a most probable value and β is the coefficient which characterises non-idealities at the interface between R and C and characterises a surface roughness [17]. A β value of unity is equivalent to a perfectly smooth surface with no surface roughness. ω_0 is a correction factor for units and is always set to unity. C_{inf} or the *ZFC* of the monolayer relates to the thickness of the monolayer, d, and the relative dielectric constant, ε, by the equation [19]:

$$ZFC = C = \frac{\varepsilon_0 \varepsilon}{d}$$

where $\varepsilon_0 = 8.84 \times 10^{-8}\,\mu F\,cm^{-1}$ and is the dielectric constant of a vacuum.

As a result an increase in the capacitance of the monolayer relates either to a decrease in its thickness or an increase in its relative dielectric constant. In either case, the capacitance of a monolayer is very sensitive to its structure.

3. Results

Figure 1(a) displays Cole–Cole plots in the complex capacitance plane derived from impedance data of ***ssm*** coated mercury electrodes. The plot for DOPC coated electrodes is shown for comparison as a single semicircle which corresponds to a simple capacitor in series with a resistor. The plots for the ***ssm*** coated mercury

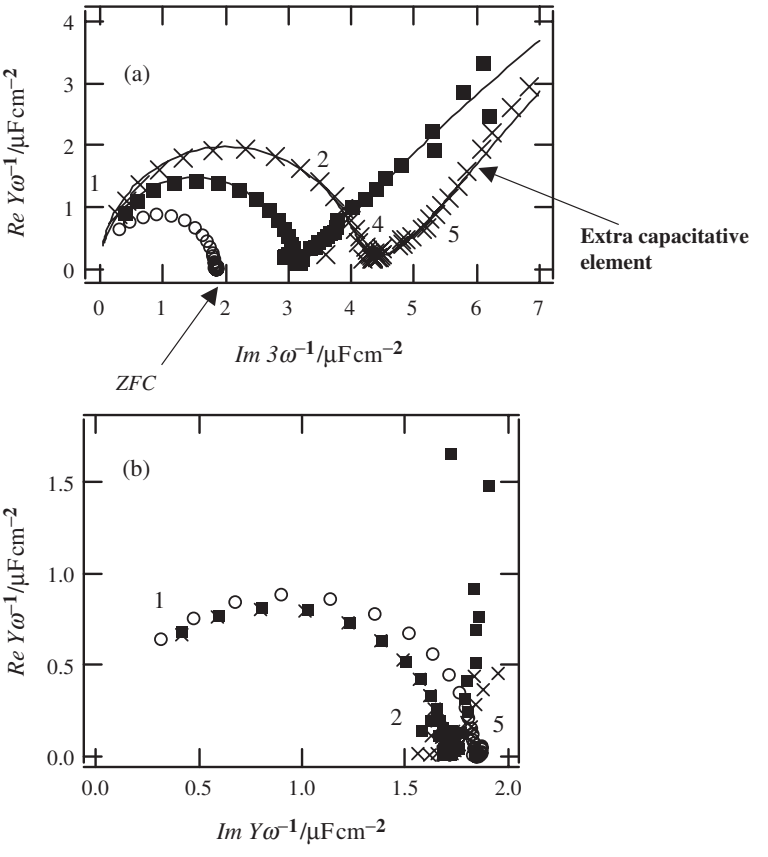

Figure 1. Plots in complex capacitance plane of impedance data derived from (a) dcm ***ssm*** (crosses, extra capacitative element indicated), hexane ***ssm*** (filled squares) and DOPC monolayer (open circles, *ZFC* indicated) and (b) DOPC-33% dcm ***ssm*** (crosses), DOPC-33% hexane ***ssm*** (filled squares) DOPC monolayer (open circles) coated mercury in 0.1 mol dm^{-3} KCl. In (a) equation (1) fit as solid line. Numbers on plots indicate frequencies of adjacent data points expressed as and representing values in log (ω/rad s^{-1}) as follows: 1, 5.61; 2, 4.42; 4, 2.05 and 5, 0.87.

electrodes show a significant extra element in addition to the *RC* semicircle. The fits of equation (1) to the data are good. The *ZFC* of the plot derived from data for the hexane ***ssm*** coated electrode is lower (~3 μF cm^{-2}) than that derived from data for the dichloromethane (dcm) ***ssm*** layer coated electrode (~4.5 μF cm^{-2}).

Figure 1(b) displays Cole–Cole plots in the complex capacitance plane derived from impedance data of the DOPC-33% ***ssm*** coated mercury electrode. The plot derived from data for the DOPC coated electrode is shown for comparison. Only the plots from data for DOPC-hexane ***ssm*** coated electrodes give rise to a significant extra capacitative element in addition to the *RC* semicircle. The *ZFC* derived from the impedance data of DOPC-***ssm*** coated mercury is lower than that derived from the impedance data of DOPC coated mercury.

Figure 2(a) summarises the α coefficient values which characterise the extra capacitative element derived by fitting equation (1) to data of hexane and dcm ***ssm*** and DOPC-hexane ***ssm*** coated electrodes where the extra capacitative element is significant. The α value characterising this element is lower in impedance data derived from ***ssm***

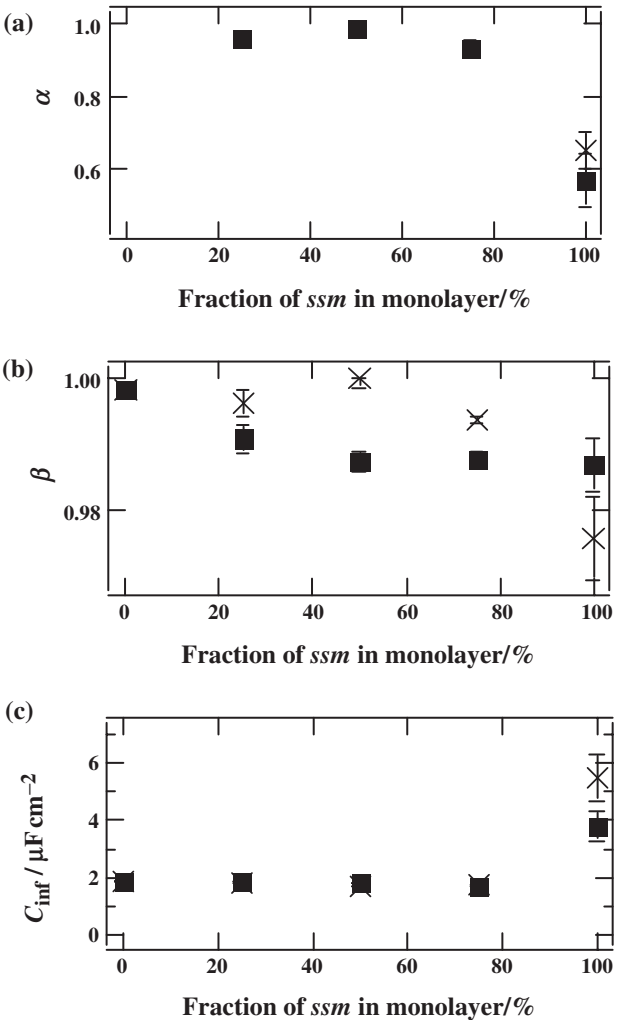

Figure 2. (a) α and (b) β values derived from fits to admittance data using equation (1) and (c) C_{inf} equivalent to *ZFC* for layer on mercury as a function of % weight fraction of dcm (crosses) and hexane (filled squares) ***ssm*** in DOPC.

coated mercury than that derived from data of DOPC-hexane ***ssm*** coated mercury. Figure 2(b) displays the value of the coefficient β obtained by fitting equation (1) to the impedance data from the coated electrodes. The data from the dcm ***ssm*** coated mercury shows a lower β value compared to that derived from data from the hexane ***ssm*** coated mercury. On the other hand, the β values derived from the DOPC-dcm ***ssm*** coated mercury are higher than those derived from the data from the DOPC-hexane ***ssm*** coated mercury. Figure 2(c) is a summary of the C_{inf} values following application of equation (1) to the impedance data. These values are equivalent to the *ZFC* values derived from the Cole–Cole plots in figures 1(a) and (b) and confirm the decreased *ZFC* of the mixed DOPC-***ssm*** layer compared to the ***ssm*** coated mercury.

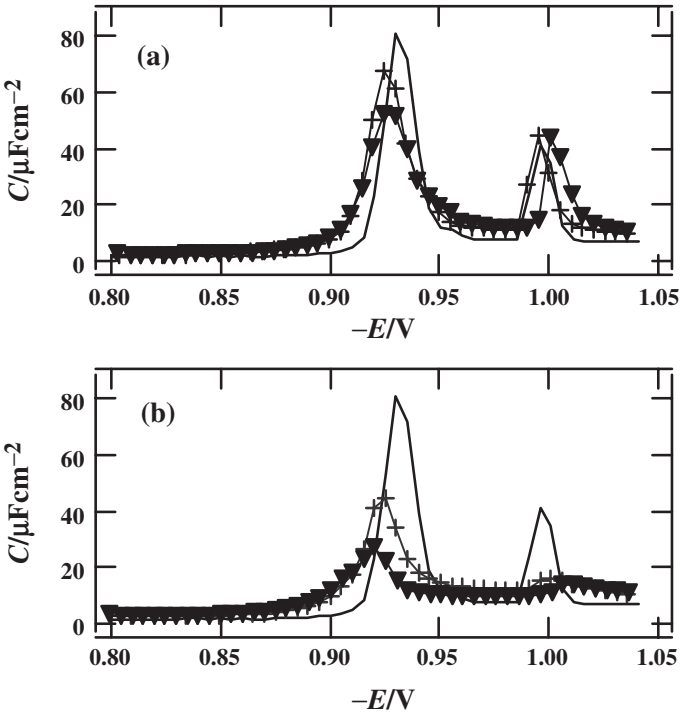

Figure 3. Capacitance–Potential plots of (a) dcm and (b) hexane ***ssm*** in DOPC at 0% (solid line) 25% (crosses) and 50% (filled triangles) weight fraction ***ssm***.

Figure 3 displays capacitance–potential (*C–E*) plots obtained from layers of DOPC and DOPC-***ssm***. The plot for the pure DOPC monolayer exhibits a flat capacity minimum at potentials corresponding to the PZC of mercury, ~ -0.4 V to -0.7 V followed by two well-defined capacitance peaks at more negative potentials. The capacitance peaks correspond to two successive phase transitions of the phospholipids [11]. These phase transitions are affected when the monolayer develops inhomogeneties or defects and the effect is manifest as a depression of the capacitance peaks [3]. Figure 3 shows that the effect of adding the ***ssm*** to DOPC is to depress the capacitance peaks representing the phase transitions of DOPC. This depression is more marked in data derived from DOPC-hexane ***ssm*** coated electrodes. Note that the general form of the *C–E* plot for DOPC is not changed even with 50% ***ssm*** mixed with the DOPC.

Figures 4(a), (b), (c) and (d) display Cole–Cole plots in the complex capacitance plane derived from impedance data of DOPC-25% ***ssm*** coated electrode exposed to 4×10^{-7} mol dm^{-3} pyrene and promethazine in solution. Figure 4(c) shows that there is a clear decrease in the zero free capacitance when the DOPC-dcm ***ssm*** layer is exposed to pyrene. A smaller decrease of the *ZFC* is seen when pyrene interacts with the DOPC-hexane ***ssm*** mixed layer (figure 4a). No decrease is seen when pyrene interacts with the pure DOPC layer. Both pyrene and promethazine introduce a second capacitative element on interaction with the DOPC-dcm ***ssm*** coated electrode (figures 4c and d).

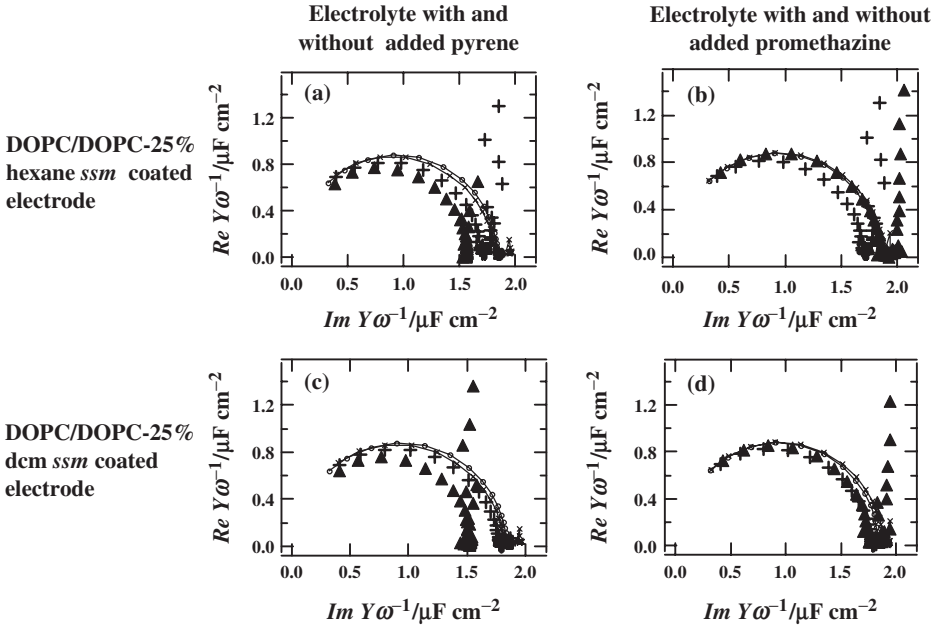

Figure 4. Plots in complex capacitance plane of impedance data derived from DOPC small open circles and DOPC-25% ***ssm*** vertical crosses coated mercury and; DOPC small diagonal crosses and DOPC-25% ***ssm*** filled triangles coated mercury with pyrene or promethazine at 4×10^{-7} mol dm^{-3} concentration in 0.1 mol dm^{-3} KCl.

4. Discussion

It has been shown previously that the impedance data derived from a DOPC coated electrode where no extra capacitative element is evident and with a β coefficient close to unity corresponds to a fluid monolayer with no structural order in the plane parallel to the electrode and no surface roughness [2]. Introduction of gramicidin peptide channels into the layer creates a structural inhomogeneity which is observed as an extra capacitative element in the impedance data and a β coefficient significantly lower than unity [2, 3]. It follows from this therefore that the impedance data derived from layers of ***ssm*** on the mercury electrode (figure 1) shows that (i) they are inhomogeneous as indicated by the presence of a significant extra capacitative element and (ii) they possess a surface roughness shown by a value of β significantly less than unity.

Comparing the data of the hexane ***ssm*** and dcm ***ssm*** coated electrodes, the lower value of C_{inf} or ZFC derived from the data of the hexane ***ssm*** coated electrode concurs with a more condensed layer on the mercury and is in line with the material's non-polar properties compared to the polar dcm ***ssm***. Interestingly the hexane ***ssm*** layer has a lower surface roughness (higher β) than the dcm ***ssm*** layer which has also been shown in BAM imaging measurements of a similar layer at the air–water interface [20]. The decreased roughness of the hexane ***ssm*** extract layer could arise from the fact that the hexane ***ssm*** forms a more condensed layer.

The impedance data of the mixed layers indicate that the characteristics of the DOPC dominate the mixed layer. The value of C_{inf} or ZFC is slightly lower than that of the

DOPC layer on mercury (figure 2c) for mixtures of all proportions. This is consistent with the ***ssm*** being segregated in the polar head region of the DOPC monolayers. The occurrence of a significant extra capacitative element in the data derived from mixed DOPC-hexane ***ssm*** layers figure 1(b) concurs with an inhomogeneous layer due to some incompatibility of the DOPC layer and the non-polar hexane extract. The increased value of α may be attributed to the nature of the defects which are characteristic of the DOPC-***ssm*** mixing and not the properties of the hexane ***ssm***. The polar dcm ***ssm*** when mixed with the DOPC forms monolayers with decreased inhomogeneity compared to the hexane ***ssm***-DOPC layers as shown by a higher β value in figure 2(b) and no significant extra capacitative element. The *C–E* plots obtained from mixed layer coated electrodes are also interesting (figure 3). The similarity of the form of the plots confirms that the capacitance or dielectric properties of the layers are determined by those of DOPC. The depression of the capacitance peaks, which is more pronounced in *C–E* curves of the DOPC-hexane ***ssm*** mixed layers, indicates the increased inhomogeneity of the DOPC-hexane ***ssm*** layers [3]. This is in accord with the conclusions from the impedance data. The segregation of the ***ssm*** in the DOPC polar head region would explain why mixtures of DOPC and the non-polar hexane ***ssm*** layers show greater structural inhomogeneity than mixtures of DOPC and the polar dcm ***ssm*** layers.

In figure 4, the values of the *ZFC* on exposure of the DOPC-hexane ***ssm*** mixed layer and the DOPC-dcm ***ssm*** mixed layer with pyrene indicate a significant association of pyrene with the dcm ***ssm*** component. This is also in accord with the ***ssm*** residing in the polar head region where it is more available for association with pyrene in the solution phase. It is interesting also that both pyrene and promethazine interact with the DOPC-dcm ***ssm*** mixed layer and introduce defects into the layer shown as an extra capacitative element. Studies on this aspect are continuing.

5. Conclusions and future direction

The main findings from this article are that layers of extracted ***ssm*** on a mercury electrode show a structural inhomogeneity compared to layers of DOPC on a mercury electrode. Further, in mixtures of the extracted ***ssm*** with DOPC on the mercury electrode, the ***ssm*** appears to reside in the polar head region of DOPC.

This study has shown that EIS can be used as an additional means to understand the physical and chemical properties of extracted surface layers. The interaction of ***ssm*** with well-characterised insoluble surfactants such as phospholipids and hydrophobic materials in solution can be studied using these methods. Future work will correlate these results with the chemical analysis of the ***ssm*** and develop the impedance techniques for studying the ***ssm*** *in situ*. At present, the results give information on the polarity and structural homogeneity of the microlayer and provide a method of distinguishing different microlayer samples. Multivariate analytical (mva) techniques which have already been applied successfully to analyse impedance data from supported layers can be used to quantify the data and objectively characterise the interactions within the ***ssm*** [21, 22]. The power of the mva technique is that when it is used with other methods, molecular characteristics of the microlayer can be identified with characteristics of the impedance spectra. These calibrations can be then used to identify molecular properties of the microlayer from impedance data obtained *in situ*.

Acknowledgements

This work was funded by the ALIS programme of the British Council and the Ministry of Science, Education and Sport of the Republic of Croatia. Thanks to Blaženka Gašparović (RBI) for very helpful comments.

References

[1] P.S. Liss, R.A. Duce. *The Sea Surface and Global Change*, Cambridge University Press, Cambridge, United Kingdom (1997).
[2] C. Whitehouse, R. O'Flanagan, B. Lindholm-Sethson, B. Movaghar, A. Nelson. *Langmuir*, **20**, 136 (2004).
[3] C. Whitehouse, D. Gidalevitz, M. Cahuzac, R.E. Koeppe II, A. Nelson. *Langmuir*, **20**, 9291 (2004).
[4] W.D. Garrett. *Limnol. Oceanogr.*, **10**, 602 (1965).
[5] B. Ćosović, V. Vojvodić. *Mar. Chem.*, **22**, 363 (1987).
[6] Z. Kozarac, B. Ćosović, S. Frka, D. Möbius, S. Hacke. *Colloid Surf. A: Physicochem. Eng. Asp.*, **219**, 173 (2003).
[7] G.L. Gaines Jr. *Insoluble Monolayers at Liquid–Gas Interface*, Wiley, New York (1966).
[8] S. Frka, Z. Kozarac, B. Cosovic. *Rapp. Comm. Int. Mer Medit.*, **37**, 198 (2004).
[9] K. Hayase, H.J. Tsubota. *Colloid Interface Sci.*, **114**, 220 (1986).
[10] W.R. Barger, J.C. Means. In *Marine and Estuarine Geochemistry*, A.C. Sigleo, A. Hattori (Eds), p. 47, Lewis Publishers, Chelsea, United Kingdom (1985).
[11] D. Bizzotto, A. Nelson. *Langmuir*, **1**, 6269 (1998).
[12] A. Nelson. *Biophysical J.*, **80**, 2694 (2001).
[13] G. Wiegand, N. Arribas-Layton, H. Hillebrandt, E. Sackmann, P. Wagner. *J. Physi. Chem. B*, **106**, 4245 (2002)
[14] R.P. Janek, W.R. Fawcett, A. Ulman. *J. Phys. Chem.* B. **101**, 8550 (1997).
[15] B. Lindholm-Sethson. *Langmuir*, **12**, 3305 (1996).
[16] L. Strašák, J. Dvořák, S. Hason, V. Vetterl. *Bioelectrochemistry*, **56**, 37 (2002).
[17] P. Peng Diao, D. Jiang, X. Cui, D. Gu, R. Tong, B. Zhong. *J. Electroanal. Chem.*, **464**, 61 (1999).
[18] S. Lingler, I. Rubinstein, W. Knoll, A. Offenhausser. *Langmuir*, **13**, 7085 (1997).
[19] A.J. Bard, L.R. Faulkner. *Electrochemical Methods*, p. 501, John Wiley and Sons, New York, USA (1980).
[20] Z. Kozarac, D. Risović, S. Frka, D. Möbius. *Mar. Chem.*, **96**, 99 (2005).
[21] B. Lindholm-Sethson, P. Geladi, A. Nelson. *Anal. Chimi. Acta*, **446**, 121 (2001).
[22] B. Lindholm-Sethson, J. Nystrom, P. Geladi, A. Nelson. *Anal. Bioanal. Chem.*, **375**, 350 (2003).